J. Fluid Mech (1988), *vol.* 191, *pp.* 225–245
Printed in Great Britain

Flow structure from an oscillating cylinder Part 2. Mode competition in the near wake

By A. ONGOREN AND D. ROCKWELL
Department of Mechanical Engineering and Mechanics, Lehigh University, Bethlehem, PA 18015, USA

(Received 10 July 1986 and in revised form 1 September 1987)

A circular cylinder subjected to forced oscillations at angle α with respect to the free stream shows a number of admissible modes of vortex formation synchronized with the body motion. These modes can be categorized into two basic groups: symmetrical vortex formation; and antisymmetrical vortex formation. Whereas there is a single symmetrical mode, there are four basic antisymmetrical modes. Three of these antisymmetrical modes show period doubling relative to the classical Kármán mode. This doubling arises from the symmetrical perturbation component induced by the cylinder motion at $\alpha \neq 90°$. Synchronization, i.e. phase-locking of the vortex shedding with the cylinder motion, is possible for all of these modes. It occurs even when streamwise ($\alpha = 0°$) motion induces an antisymmetrical mode.

When synchronization does not occur, there is competition between the symmetrical and antisymmetrical modes; the near-wake structure successively locks-on to each mode over a defined number of cycles, abruptly switching between modes. The number of occurrences of each mode is a well-defined function of excitation frequency and angle α.

If, in contrast to steady-state motion of the cylinder, there is an initial transient motion, the transition between symmetrical and antisymmetrical modes has a markedly different character, emphasizing the importance of initial conditions. Abrupt onset of sinusoidal motion produces an initially synchronized symmetrical mode, which gradually decays to an antisymmetrical mode. The number of excitation cycles to onset of decay to antisymmetrical mode is highly repeatable. Moreover, the mechanism of decay of the near wake from the symmetrical to antisymmetrical mode can occur deterministically over a defined number of cycles.

1. Introduction

In Part 1 (Ongoren & Rockwell 1988), we have addressed features of the near-wake structure for excitation of the cylinder in the cross-stream direction. As described therein, synchronized antisymmetrical vortex formation and interaction can occur; synchronization corresponds to phase-locking of the vortex formation with respect to the cylinder motion.

In the event that the cylinder is forced in a direction other than the cross-stream direction, the issue arises as to whether there are other synchronized modes of shedding, and under what conditions they occur. Griffin & Ramberg (1976) show a number of persistent patterns of asymmetrical vortex-street formation due to in-line oscillation. In addition, a variety of observations of vortex patterns arising from in-line motion are summarized and assessed by Naudascher (1986).

In general, for cylinder excitation in the streamwise ($\alpha = 0$), i.e. in-line, direction,

the perturbation produced by the cylinder will be a symmetrical one, while the naturally occurring mode of large-scale vortex formation and its upstream influence is antisymmetrical. Consequently, one expects, in general, competition between the symmetrical and antisymmetrical modes; under certain conditions, one mode may prevail, producing synchronization of the near-wake flow structure with the cylinder motion.

Furthermore, if the cylinder is excited at an angle other than the cross-stream ($\alpha = 90°$) or streamwise ($\alpha = 0°$) direction, then there is mixed-mode excitation: the perturbation from the cylinder motion contains both symmetrical and antisymmetrical contributions and the potential for exciting both types of modes. It may be possible for one of the modes to emerge as the dominant one, again producing a synchronized near-wake structure such that the instantaneous flow structure locks to the body motion. In general, when there is not synchronization in the near-wake, the mode competition will most likely produce switching back and forth between the basic modes of vortex formation. The degree of intermittency of this switching, as well as the typical frequency of switching, are central features that have yet to be characterized.

Finally, in the event that a stationary cylinder is abruptly set into sinusoidal motion, as opposed to the foregoing steady-state sinusoidal excitation, one expects initial dominance of the mode produced by the cylinder motion, with subsequent persistence of this mode, or decay to another mode. When such decay does occur, it may well be in a deterministic fashion, thereby lending further insight into the coexistence of, and competition between, modes of vortex formation.

In this investigation, we address these issues of synchronized and competing modes of vortex formation, with the primary objective of determining the instantaneous flow structure in relation to the body motion.

2. Experimental system and instrumentation

Essentially the same experimental techniques and instrumentation were employed as in Part 1. Excitation at arbitrary angle α was achieved by rotating the entire forcing system, including the motor and gear arrangement, to the desired angle α.

The inset of figure 1 shows a schematic representing cylinder oscillations at an angle α with respect to the free stream. Oscillation amplitude is defined as X_e and η_e for $\alpha = 0°$ and $\alpha > 0°$ respectively. For most experiments, a constant value of dimensionless amplitude $X_e/D = \eta_e/D = 0.13$ was chosen; exceptions are noted in the text. Preliminary studies showed that this amplitude was sufficiently large to produce control of the near-wake structure over a wide frequency range. The frequency of excitation f_e relative to the natural vortex-shedding frequency f_0^* from the corresponding stationary cylinder took values in the range $0.5 \leqslant f_e/f_0^* \leqslant 4.0$; this excitation range allowed examination of the modal structure of the near wake for sub- and superharmonic excitation. Particularly important in addressing the concept of mode competition is definition of the mode of the near wake from that of the corresponding stationary cylinder. As discussed in detail in Part 1, the large-scale, self-excited instability from the stationary cylinder was in the purely antisymmetric mode for these experiments.

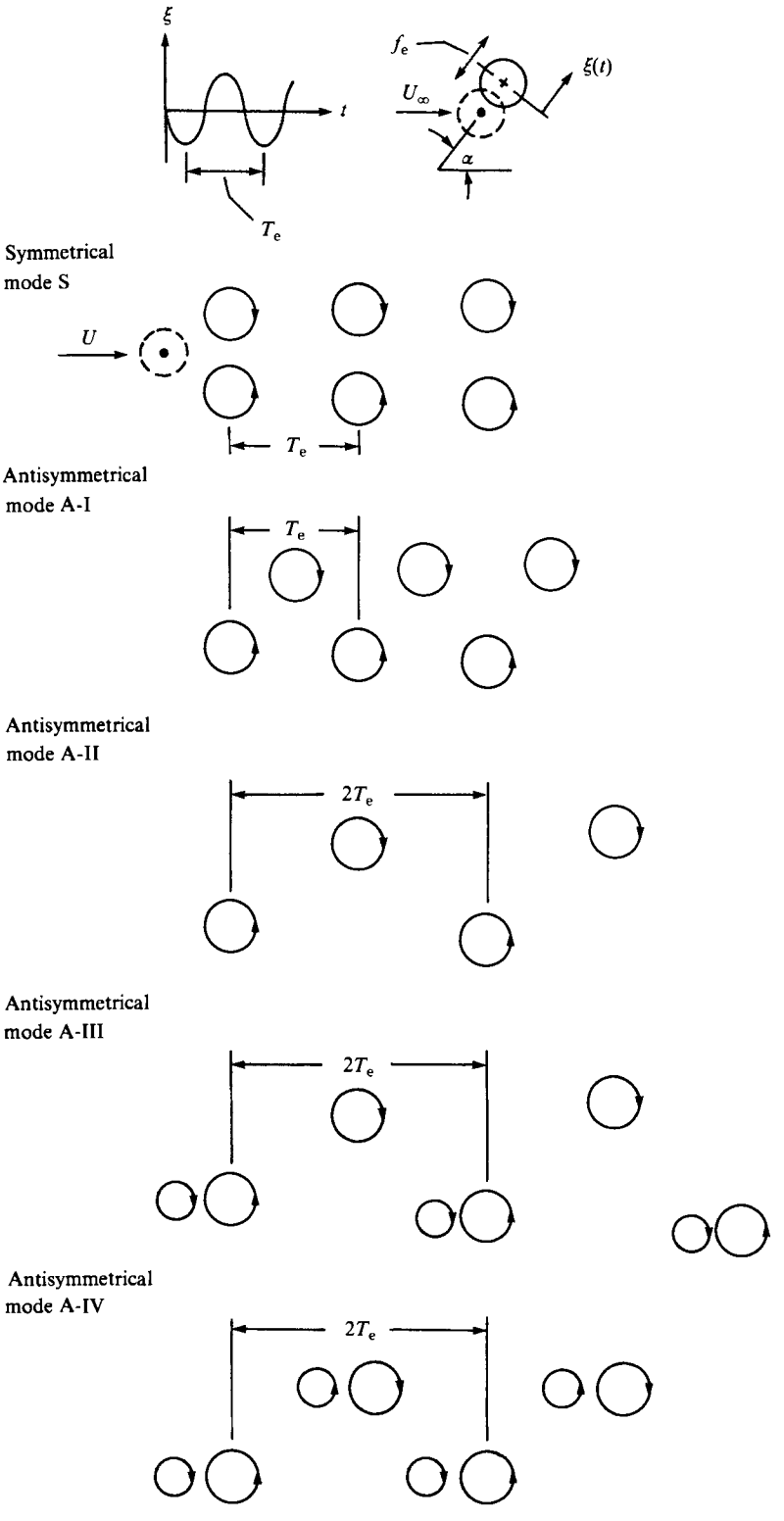

FIGURE 1. Representation of basic modes of vortex formation from cylinder oscillating at angle α with respect to free stream.

3. Overview of basic modes

As a result of extensive flow visualization, it is evident that a number of possible modes of vortex shedding can be synchronized with the cylinder motion. Moreover, even when synchronization does not occur, two of these fundamental modes tend to compete with each other, with switching back and forth between them. Before proceeding with details, it is helpful to define each of these modes, schematically portrayed in figure 1. Therein, the sketches illustrate the time history of the vortex formation in the near wake. The precise details of the vortex shedding from the cylinder and the mutual interaction near the cylinder are complex for certain of the higher-order modes; they will be defined subsequently.

For cylinder oscillations at angle α with respect to the free stream, the modes of vortex formation can be categorized into two basic groups: a symmetrical mode of vortex formation, denoted as S and antisymmetrical modes of vortex formation denoted as A. For the symmetrical mode, a pair of vortices is shed in phase from both sides of the cylinder during one oscillation cycle. The antisymmetrical mode appears in four forms: A-I, A-II, A-III and A-IV. In the case of the A-I mode, there is alternate, out-of-phase shedding of vortices from either side of the cylinder over an oscillation cycle; this is the classical mode of vortex shedding leading to formation of the Kármán street. For modes A-II to A-IV, the period of the vortex pattern is $2T_e$, as opposed to T_e for the classical A-I mode; moreover, modes A-III and A-IV involve formation of counter-rotating vortex pairs.

On the basis of our experiments, it is possible to describe some general conditions for occurrence of each of the foregoing modes. Mode S can occur at any value of excitation angle α, except $\alpha = 90°$; that is, if there is a symmetrical component in the perturbation imparted by the cylinder to the flow, self-selection and predominance of a synchronized S mode can occur. Modes A-II–A-IV occur only for $0° \leqslant \alpha < 90°$ where there is a symmetrical component in the flow perturbation; evidently, as shown in the schematic, the effect of this symmetrical component of the perturbation is to double the period of the antisymmetrical vortex formation. This period doubling arises from the fact that shedding of two successively antisymmetrical vortices, or vortex combinations, from a cylinder oscillating in the streamwise direction requires two cycles of cylinder motion; in contrast, only one cycle of cylinder oscillation in the cross-stream direction is required. As a further refinement on our generalization, we note that mode A-II occurs only for $\alpha \neq 0°$ corresponding to simultaneous excitation in symmetrical and antisymmetrical modes. Modes A-III and A-IV occur only for $\alpha = 0°$. We emphasize that the generalizations for occurrence of these modes are restricted to the relatively small amplitudes of the cylinder oscillation addressed herein.

In the following, we determine the conditions for which these modes occur, for both synchronized and non-synchronized vortex formation.

4. Mode synchronization and mode competition due to steady-state excitation

4.1. *Preferred and synchronized modes of vortex formation*

Figure 2 shows the representative wake structure for streamwise ($\alpha = 0°$) oscillations of the cylinder. All photos correspond to the maximum upstream $x = -X_e$ position of the cylinder. There are two synchronized modes, one occurring at $f_e/f_0^* = 2$,

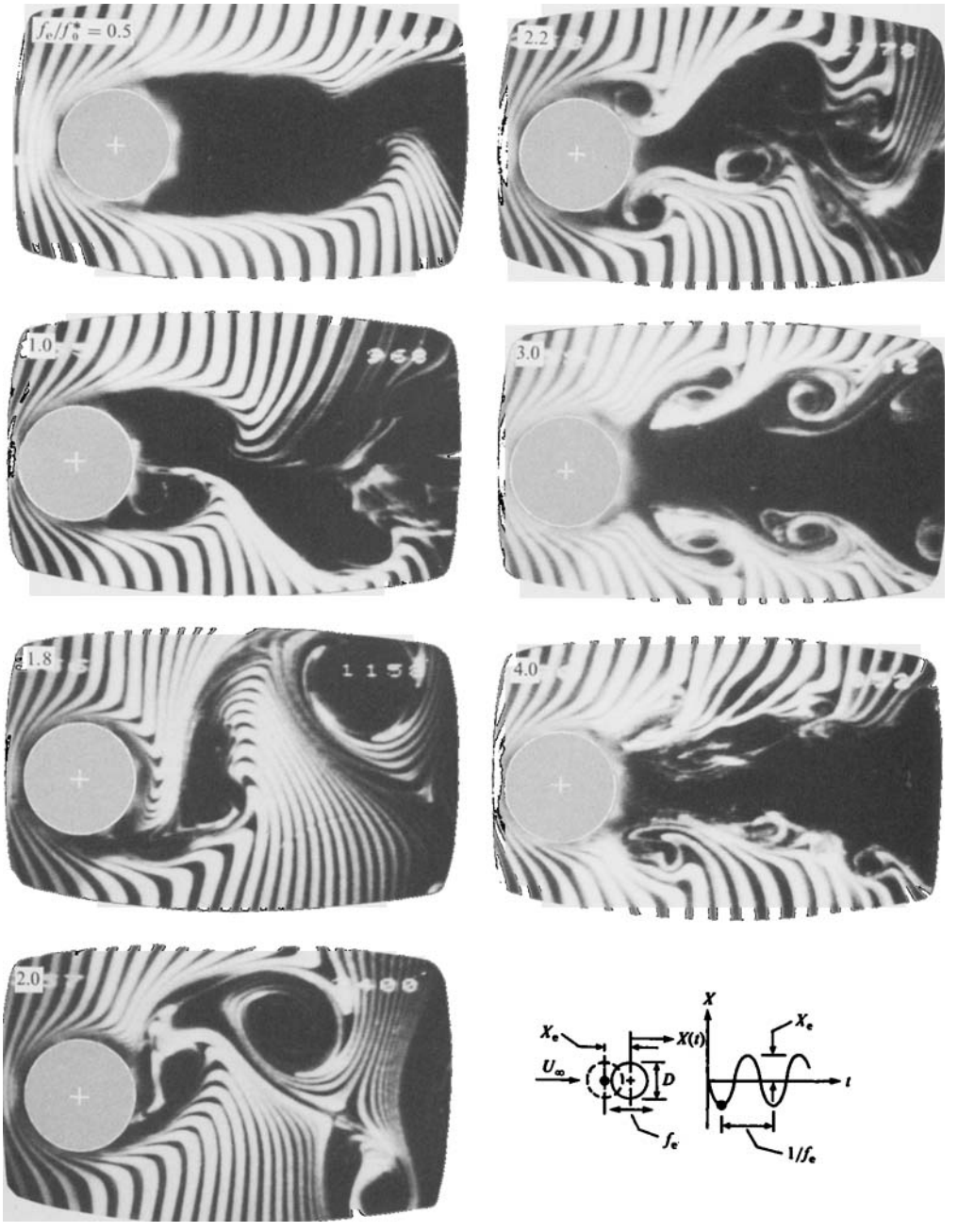

FIGURE 2. Preferred modes of near-wake structure for various ratios of excitation frequency f_e of cylinder to vortex shedding frequency f_0^* from corresponding stationary cylinder. All photos taken at instant when cylinder is in maximum upstream position during oscillation cycle.

corresponding to mode A-III in figure 1; and the other at $f_e/f_0^* = 3$, designated mode S in figure 1.

The photo at $f_e/f_0^* = 2$ shows, in its right-hand portion, two vortices of like sense originally shed from the upper side of the cylinder; a single vortex of opposite sense is about to form from the lower side. In the photo at $f_e/f_0^* = 3$, the symmetrical

vortex arrangement (mode S) persists for at least three vortex pairs in the downstream direction. Moreover, similar synchronization persists at $f_e/f_0^* = 4$ as well, though the vortices rapidly lose their coherence after the first pair is formed. These synchronized patterns at $f_e/f_0^* = 2$, 3, 4 remain the same over a very large number of oscillation cycles.

At all other values of excitation frequency in figure 2, there is mode competition and switching between symmetrical and antisymmetrical vortex formation, with the preferred mode shown in each photo; by 'preferred mode' we mean that mode which tended to occur most often over a run of hundreds of cycles. This mode competition will be quantified subsequently. There is, as shown in figure 2, a general trend of these preferred modes with increasing f_e/f_0^*. In essence, at lower values of excitation frequency the antisymmetrical mode tends to occur, while at higher values there is a tendency for onset of the symmetrical mode. Particularly interesting is the case of $f_e/f_0^* = 2.2$; there is initial vortex formation in a nearly symmetrical mode, which rapidly decays to an antisymmetrical mode shortly downstream of the cylinder.

The time-dependent flow structure corresponding to the synchronized vortex formation in mode A-III (at $f_e/f_0^* = 2$) is detailed in figure 3; it shows the flow structure over one complete cycle of oscillation. Vortex shedding from the upper side of the cylinder is initiated in photo (*a*), taken at the maximum negative (upstream) position of the cylinder. As the cylinder moves downstream, the shed layer moves down and away from the downstream portion of the cylinder, completing the shedding of the first vortex. The second vortex is formed as the cylinder passes through its maximum positive (downstream) position and changes direction. This shedding of two vortices from the upper side is then followed by formation of a single vortex from the lower side, indicated in photo (*g*); the completion of this single vortex formation and its downstream convection are shown in photos (*a*)–(*e*). During a typical experimental run extending over 50 cycles or so, the shedding of the two vortices from the upper side of the cylinder persisted from that same side. However, by bringing the flow to rest, then to full speed again, it is possible to obtain mirror images of the patterns shown in figure 3.

As noted in the foregoing, excitation at frequencies for which there is no synchronization produces switching between symmetrical and antisymmetrical modes of vortex shedding. Figure 4 compares these modes for selected values of f_e/f_0^*. The preferred modes at each value of f_e/f_0^* have already been given in figure 2. Of course, in cases where the oscillations are synchronized, only the antisymmetrical ($f_e/f_0^* = 2$) or symmetrical ($f_e/f_0^* = 3, 4$) mode of vortex formation occurs. In the photos corresponding to $f_e/f_0^* = 0.33$ and 0.5, the vortex formation length remains virtually unaffected despite the mode competition. The antisymmetrical mode is of type A-I in both cases, i.e. the form of the vortex shedding is similar to that of the transversely excited cylinder. At $f_e/f_0^* = 1$, the synchronization frequency for transverse oscillations, corresponding photos illustrate that the formation length becomes extremely short for both symmetrical and antisymmetrical modes. In the symmetrical mode, vortex formation draws irrotational fluid along the wake centreline towards the cylinder base. The antisymmetrical mode is of the A-I type. At $f_e/f_0^* = 2.2$, as will be shown, the mode competition is not as pronounced as in the previous cases because the excitation is close to the synchronization case $f_e/f_0^* = 2$ (see figure 3); moreover, the scale of the shed vortices is significantly smaller in comparison with the larger-scale vortex eventually recovered in the downstream region of the flow. The left-hand photo shows the symmetrically shed vortices immediately behind the cylinder; on the right of this same photo we see the

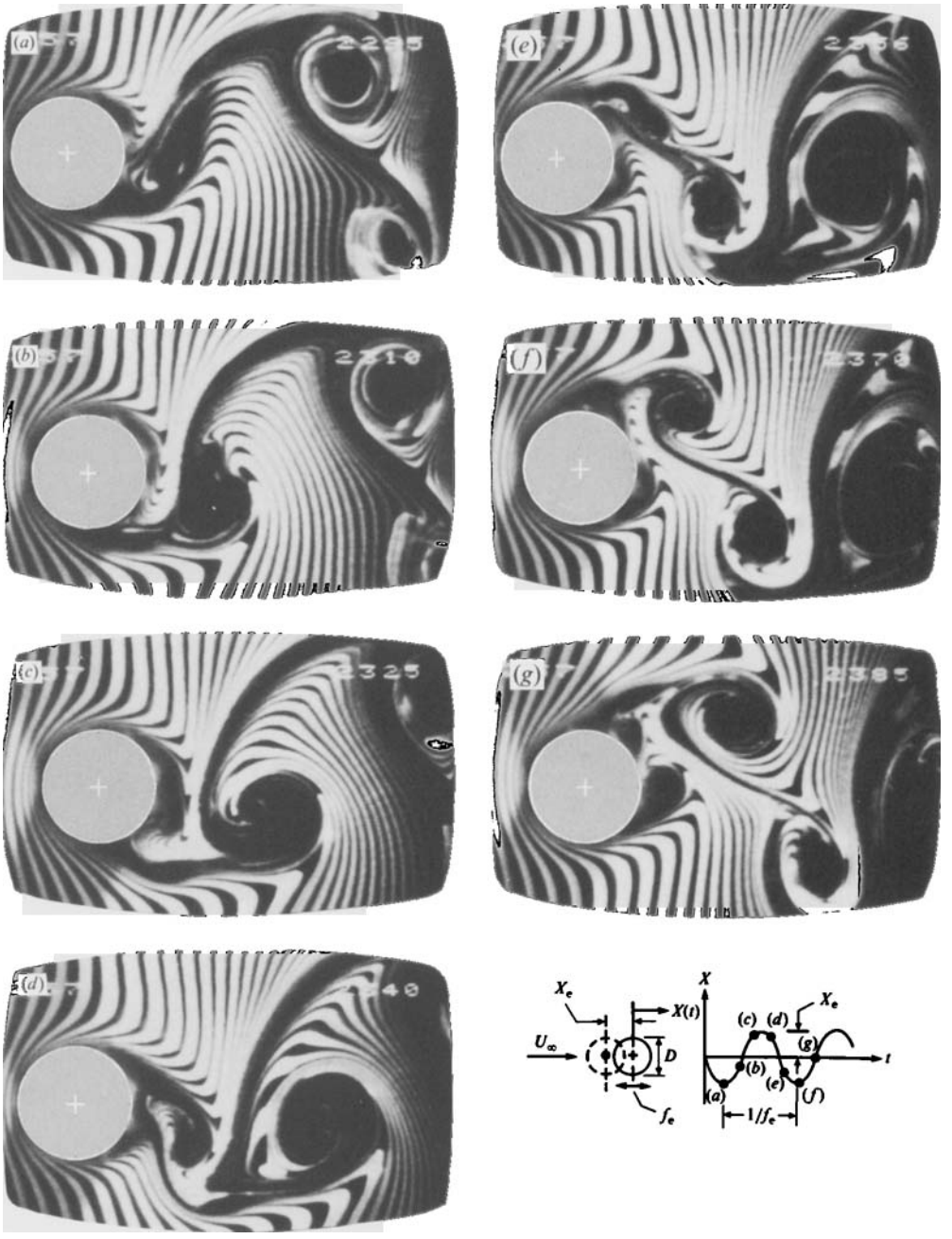

FIGURE 3. Time sequence of synchronized vortex shedding arising from cylinder oscillations in streamwise direction at frequency ratio $f_e/f_0^* = 2$. All photos taken at instant corresponding to maximum upstream position of cylinder.

recovered vortex which is the first vortex in the antisymmetric vortex street. The photo on the right, however, resembles the antisymmetrical shedding in the A-III mode (figure 3). At $f_e/f_0^* = 3$, shedding is synchronized in the symmetrical S mode. The vortices forming at frequency f_e preserve their symmetry for a long distance downstream; two pairs of symmetrical vortices are shown.

FIGURE 4. Comparison of symmetrical (left-hand column) and antisymmetrical (right-hand column) modes of non-synchronized vortex shedding from cylinder oscillating in streamwise direction as function of ratio of cylinder excitation frequency f_0^* from corresponding stationary cylinder. At $f_e/f_0^* = 3$, vortex shedding is synchronized in symmetrical mode. All photos taken at instant corresponding to maximum upstream position of cylinder during oscillation cycle.

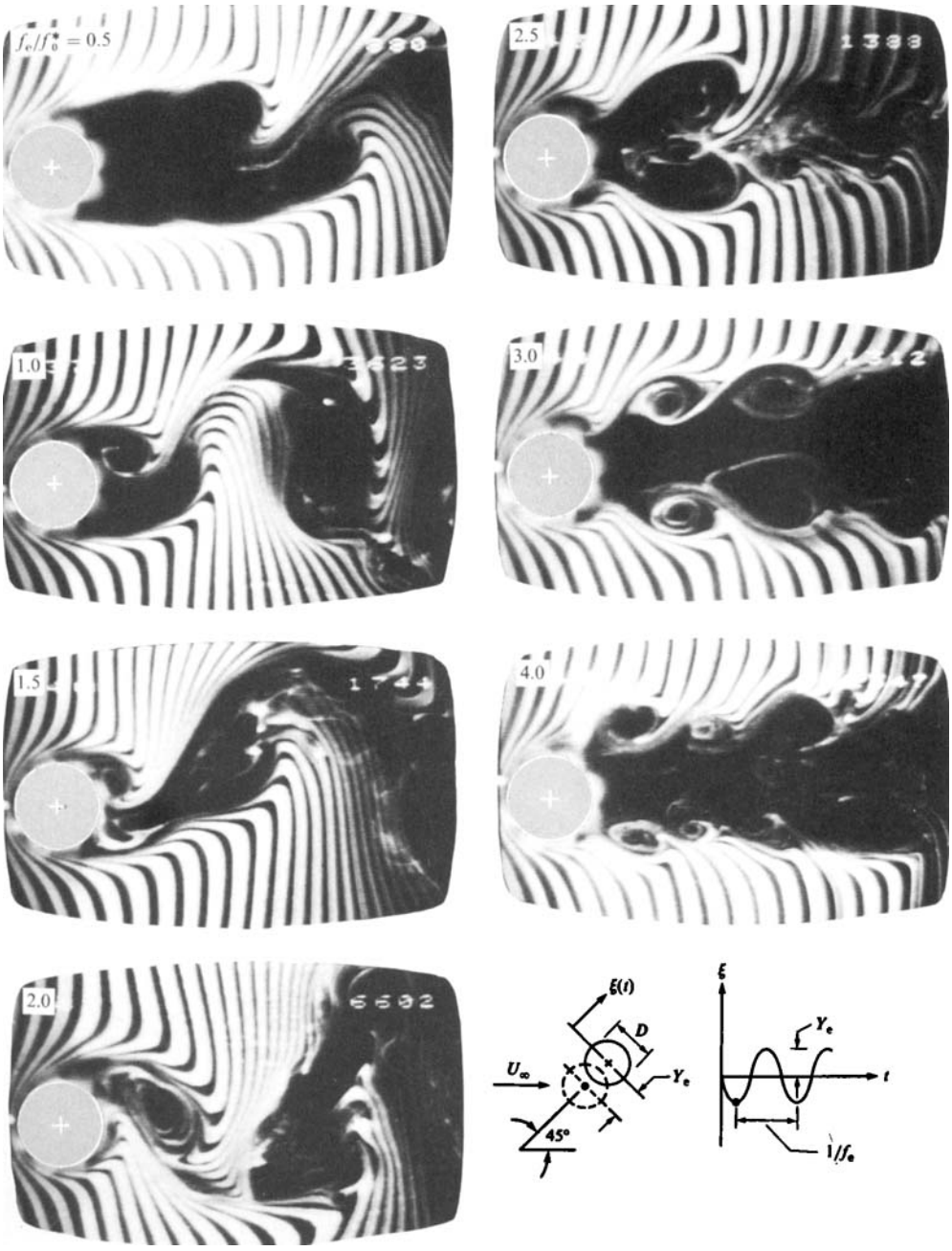

FIGURE 5. Flow structure from cylinder oscillating at angle of 45° ($\alpha = 45°$) with respect to free stream as function of ratio of excitation frequency f_e to shedding frequency f_0^* from corresponding stationary cylinder. All photos taken at position corresponding to maximum negative displacement of cylinder.

FIGURE 6. Overview of preferred modes of vortex shedding from cylinder oscillating at angles $\alpha = 0°$, 45°, 60° and 90° with respect to free stream as function of ratio of cylinder excitation frequency f_e to naturally occurring vortex shedding frequency f_0^* from corresponding stationary cylinder. All photos taken at instant corresponding to maximum negative displacement (maximum upstream position) of cylinder during oscillation cycle.

4.2. *Self-selection of modes of vortex formation in the presence of mixed-mode cylinder excitation*

Excitation of the cylinder at angles of $\alpha = 45°$, 60° and 90° was also carried out. Unlike the case of streamwise ($\alpha = 0°$) oscillations of the cylinder, where perturbations produced by the cylinder are strictly in the symmetrical mode, oscillation of the cylinder at an angle α with respect to the streamwise direction (i.e. at $\alpha \neq 0°$, 90°) induces simultaneous symmetrical and antisymmetrical perturbations. Depending upon the inherent instability mode of the near wake at a given value of excitation frequency, and the nature of the upstream influence, we expect there to be self-selection of the preferred antisymmetrical or symmetrical mode of vortex formation. Figure 5 shows representative photos of the preferred modes of the near-wake structure for cylinder oscillations at $\alpha = 45°$. At relatively low excitation frequency, $f_e/f_0^* \leqslant 2$, the wake selects the antisymmetrical A-II mode as the predominant one. At higher excitation frequency, $f_e/f_0^* \geqslant 2.5$, there is selection of the symmetrical mode.

As will be discussed subsequently (in conjunction with figure 6), synchronization of the structure of the near wake with the cylinder motion occurs at $f_e/f_0^* = 3$ and 4; moreover, synchronization is nearly achieved at $f_e/f_0^* = 1$. At all other excitation frequencies there is strong competition between modes, and switching between them.

4.3. *Overview of preferred modes of vortex formation*

Figure 6 shows an overview of the preferred modes for not only $\alpha = 0°$ and 45° as discussed in the foregoing, but also for $\alpha = 60°$ and 90°, as a function of excitation frequency f_e/f_0^*. As in the foregoing cases, all photos are taken at the maximum negative value of X_e, corresponding to maximum displacement in the upstream direction. For $\alpha = 90°$, the preferred mode is, as expected, the antisymmetrical mode A-I for all values of excitation frequency. Moreover, for subharmonic excitation $f_e/f_0^* = 0.5$, the large-scale vortex formation occurs predominantly in the antisymmetrical mode A-I for all values of α. Regarding the change in vortex formation length of this A-I mode, we compare the second row of photos with the first, i.e. $f_e/f_0^* = 1$ with $f_e/f_0^* = 0.5$. At each respective angle of excitation α, there is substantial shortening of the formation length, even for the limiting case of $\alpha = 0°$ for which there are no antisymmetrical perturbations induced by the body. Antisymmetrical mode A-II occurs at $\alpha = 45°$ and 60° for $f_e/f_0^* = 2$. Concerning the occurrence of antisymmetrical mode A-III, it occurs only at $\alpha = 0°$ for $f_e/f_0^* = 2$. Finally, referring to the photos in the bottom of figure 6, there is synchronization of the symmetrical mode S with the cylinder motion at $f_e/f_0^* = 3$ for $\alpha = 0°$, 45°, as well as at $f_e/f_0^* = 4$ for $\alpha = 0°$, 45° and 60°.

4.4. *Mode competition: characteristics of mode occurrence and switching*

Up to this point, we have spoken of the preferred mode of the near-wake structure; it is that mode which tends to occur most often over a large number of cycles. However, as emphasized in figure 4, there is switching between the preferred mode and its antisymmetrical or symmetrical counterpart. Such switching does not occur during synchronization, when the near-wake structure is phase-locked to the cylinder motion over a large number of cycles. In figures 7 and 8, we quantify the frequency of occurrence of symmetrical and antisymmetrical modes, as well as the frequency of switching between modes, as a function of excitation conditions $f_e/f_0^*$and α.

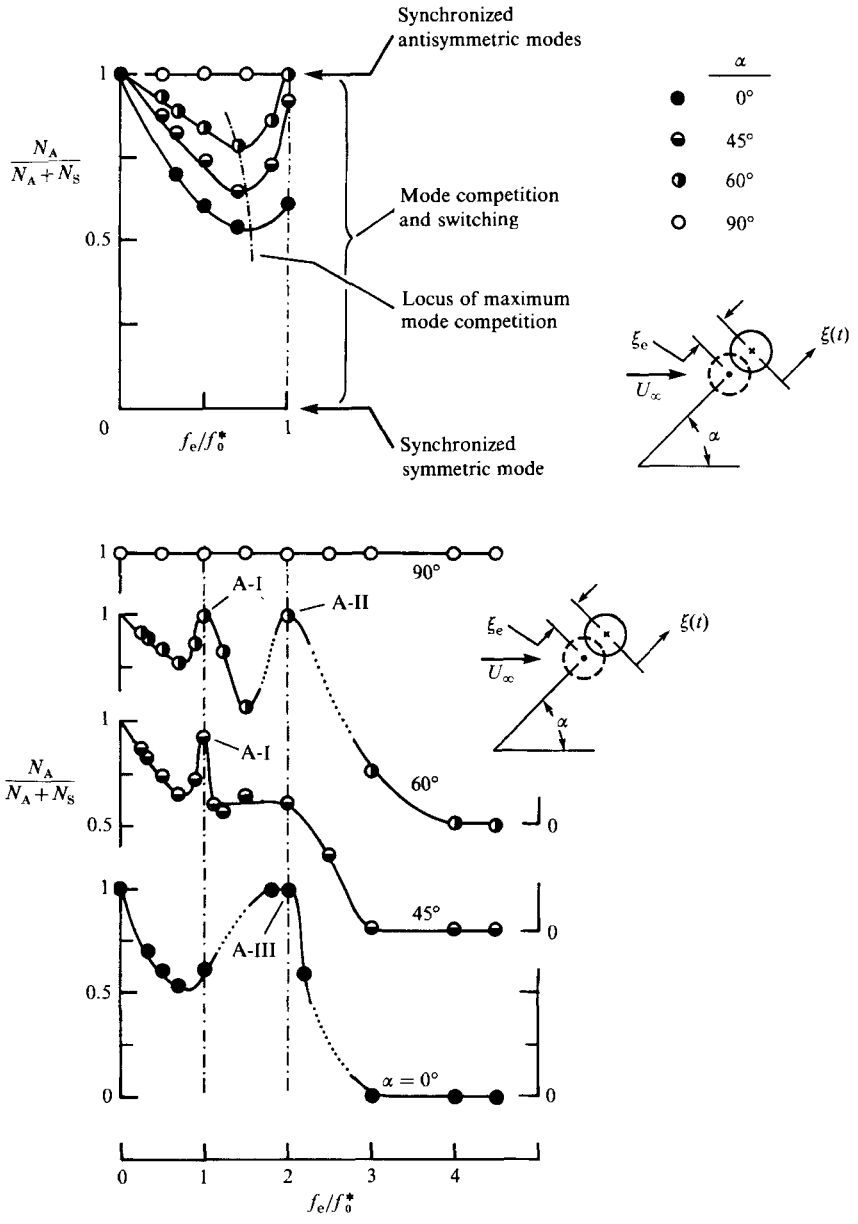

FIGURE 7. Degree of predominance of antisymmetrical mode of vortex shedding over large number of cycles as function of ratio of excitation frequency f_e to naturally occurring vortex shedding frequency f_0^* and angle of inclination α of cylinder oscillation with respect to free stream. N_A and N_S denote number of occurrences of antisymmetrical and symmetrical modes of large-scale vortex formation, and N_A+N_S denotes total number of occurrences.

Figure 7 shows the relative occurrence of antisymmetrical A and symmetrical S modes, determined from a large number of cycles of continuous, sinusoidal excitation of the cylinder. The ratio of $N_A/(N_A+N_S)$ represents the ratio of the number of cycles N_A for which either mode A-I, A-II, or A-III occurs to the total number of cycles N_A+N_S. For the extreme case of $\alpha = 90°$, the flow structure is always synchronized with the body motion and the antisymmetrical mode, therefore $N_A/(N_A+N_S) = 1$ for

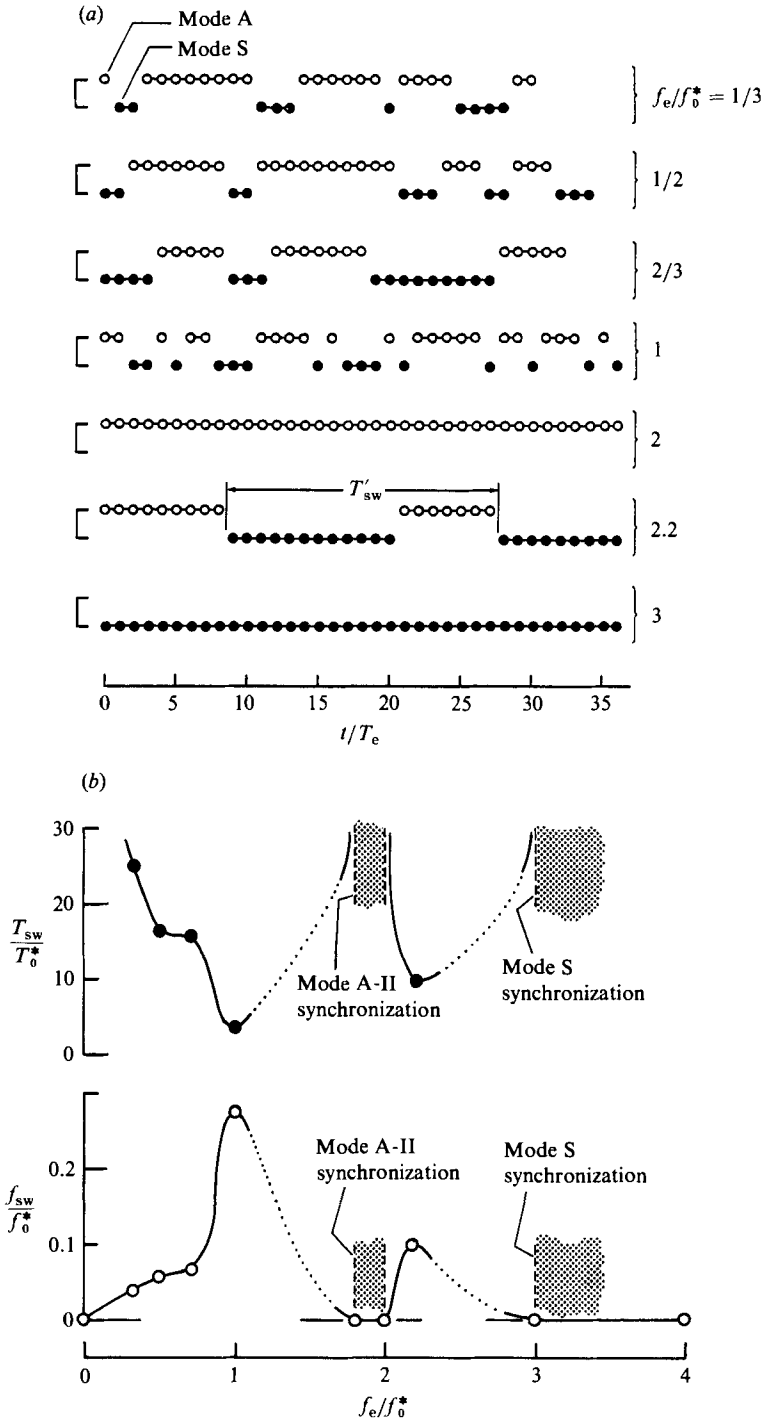

FIGURE 8. (*a*) Occurrence of antisymmetrical mode A and symmetrical mode S of large-scale vortex shedding as function of time t; T_e represents period of cylinder oscillation and T'_{sw} switching time between A and S modes. Cylinder oscillations are in streamwise direction ($\alpha = 0°$). (*b*) Variation of time-averaged switching period T_{sw} and frequency f_{sw} for cylinder oscillations in streamwise direction ($\alpha = 0°$).

all values of excitation frequency. At the other extreme, for $\alpha = 0°$, there is clearly strong competition between antisymmetrical and symmetrical modes over the frequency range of approximately $0.5 \leqslant f_e/f_0^* = 1$. For each value of $\alpha = 0°$, 45° and 60°, we interpret the minimum of each curve to represent the excitation condition for which there is maximum mode competition at a given value of α. The line passing through the curve minima is defined in figure 7 as the locus of maximum mode competition. It occurs over a frequency excitation range of approximately $0.65 \leqslant f_e/f_0^* \leqslant 0.75$. Concerning the onset of synchronization, it occurs only at $f_e/f_0^* = 1$ for $\alpha = 60°$ and 90°. It is nearly attained for $\alpha = 45°$.

Figure 7 also shows the variation of the same parameter $N_A/(N_A+N_S)$ versus excitation frequency f_e/f_0^* over the region $f_e/f_0^* > 1$. At $f_e/f_0^* = 1$, synchronization occurs in the A-I mode at $\alpha = 60°$, and nearly so at $\alpha = 45°$. At $f_e/f_0^* = 2$, synchronization occurs in the antisymmetrical mode A-II at $\alpha = 60°$ and in the antisymmetrical mode A-III at $\alpha = 0°$. No such synchronization occurs in the antisymmetrical mode for $f_e/f_0^* = 2$ at $\alpha = 45°$; apparently, there is competition such that the flow structure is not settled into either antisymmetrical mode A-I or A-III. Irrespective of angle α, there is synchronization in the symmetrical mode S at sufficiently high values of f_e/f_0^*. At $\alpha = 0°$, this synchronization in mode S sets in as early as $f_e/f_0^* = 3$.

In addition to the number of occurrences N_A and N_S, another important feature of the mode competition is the frequency of switching between antisymmetrical mode A and symmetrical mode S. Figure 8 shows an actual time representation taken for $\alpha = 0°$ for several values of excitation frequency f_e/f_0^*. Each of the data points represents a photograph taken at the maximum positive displacement of the cylinder during the cycle of oscillation; therefore, the distance between data points on the time axis represents the period of the cylinder oscillation. The switching time is defined as the time elapsed from the beginning of one mode to the end of the other; it is designated T'_{sw}. A remarkable feature of these time traces is that there is abrupt switching between antisymmetrical and symmetrical modes with each mode persisting for as long as 28 cycles. Study of the visualization shows that the flow structure of the near wake is phase-locked to the cylinder motion until it experiences a sudden jump to the other mode. Therefore, one might view the persistence of each of these modes over a defined number of cycles as short-term synchronization. We recall that for the classical type of synchronization, the structure of the wake is phase-locked to the cylinder motion over the entire experimental run.

The time-averaged switching time T_{sw} and frequency f_{sw} were obtained from consideration of hundreds of cycles of oscillation. T_0^* and f_0^* represent the period and frequency of the naturally occurring vortex shedding from the stationary cylinder. Variations of T_{sw}/T_0^*, as well as f_{sw}/f_0^*, are shown in figure 8. Occurrence of synchronization at $f_e/f_0^* \sim 2$ (in A-III mode) and at $f_e/f_0^* = 3$ (in S mode) are clearly indicated by the infinite value of switching time and the zero values of switching frequency. Maximum switching frequency occurs at $f_e/f_0^* = 1$, clearly due to the strong competition between the inherent antisymmetrical mode and the symmetrically induced perturbations due to streamwise oscillations of the cylinder.

5. Mode persistence and decay due to abrupt onset of cylinder motion

In the foregoing, we have considered steady-state excitation of the cylinder, such that the sinusoidal motion of the body and the corresponding mode of vortex formation were not influenced by the initial onset of the cylinder motion. Here we

consider the transient nature of vortex formation arising from onset of sinusoidal motion of the cylinder from its stationary position. Following this transient, the symmetrical (S) mode of vortex shedding persists over a given number of cycles, then decays.

Consider the onset of streamwise ($\alpha = 0°$) oscillations, depicted in figure 9. Sinusoidal motion abruptly starts at $t = 0$; the flow structure is examined at selected cycles, or fractions of cycles, from onset of the sinusoidal motion at constant amplitude $X_e/D = 0.3$. Figure 9 shows the response of the near wake for excitation frequencies $f_e/f_0^* = 1$, 1.5, 1.7 and 1.78, corresponding to the first–fourth columns of photos. The time from the onset of sinusoidal oscillation for each photo is indicated on the sketch. T_e is the period of the cylinder excitation, defined as $T_e = 1/f_e$.

The near wake shows similar structure at $t/T_e = 0$ (photo *a*) corresponding to the stationary cylinder, and at subsequent times, $t/T_e = 0.5$, 1.0, 1.5, ..., the corresponding photos are (*b*), (*c*), (*d*), ... Excitation at $f_e/f_0^* = 1$ shows that the near-wake structure tends to alternate between symmetrical S and antisymmetrical A modes of vortex formation. In other words, there is rapid decay of the initially induced symmetrical mode at $t/T_e = 1.0$ (photo *c*) to the antisymmetrical A-I mode at 1.5 (photo *d*), followed by a tendency to alternate between these modes.

On the other hand, at $f_e/f_0^* = 1.5$, the initially induced symmetrical S mode apparent at $t/T_e = 1$ (photo *c*) persists until $t/T_e = 2$ (photo *e*), then eventually decays the antisymmetrical mode A-III. The early stages of this decay are evident in photo (*f*); thereafter, mode A-III persists. We note, however, that this A-III mode is not synchronized at larger values of time, evidenced by the fact that the patterns of the near wake are mirror images of each other in photos (*h*) and (*i*). At higher frequency of excitation $f_e/f_0^* = 1.7$, the symmetrical mode persists for a larger number of cycles, up to photo (*g*). In photo (*i*), the antisymmetrical A-III mode is fully formed.

Finally, at the excitation frequency $f_e/f_0^* = 1.78$, the symmetrical S mode persists for an even larger number of cycles up to $t/T_e = 8.5$ (photo *h*); as will be discussed subsequently, decay to the antisymmetrical mode commences at $t/T_e = 14$ for this excitation frequency.

The fact that the decay from the highly organized and persistent symmetrical S mode shown in figure 9 at $f_e/f_0^* = 1.78$ can occur in an orderly fashion over a number of cycles is depicted in figure 10. In this sequence, we basically continue the time series shown in the right-hand column of figure 9, commenting at $t/T_e = 14$, which represents the onset of discernible antisymmetry in the symmetrical S mode. In figure 10, it is evident that with each successive cycle of the oscillation, there is increasing antisymmetry of not only the initially induced small-scale symmetrical vortex pair immediately behind the cylinder, but also in the large-scale, previously formed vortex pair shown in the right-hand portion of each photo. In photo (*f*), corresponding to the twentieth cycle after onset of transient motion, the character of the antisymmetrical mode A-II is clearly recognizable. This gradual transition between modes, which is observed for lower amplitudes ($X_e/D = 0.01$, 0.13) as well, contrasts to the abrupt switching between modes observed for steady-state excitation (see figure 8). Clearly, the initial conditions control the nature of mode transition.

Viewing figure 9 as a whole, it is evident that small changes in excitation frequency can produce a substantial increase in the number of cycles over which the symmetrical mode persists before decay into the antisymmetrical mode. The issue arises as to how deterministic this feature is; figure 11 shows the number of cycles N_S of the symmetrical mode (prior to onset of antisymmetry) as a function of excitation


$f_e/f_s = 1.78$
$f_e/f_s = 1.7$
$f_e/f_s = 1.5$
$f_e/f_s = 1$
U_∞
X_e
$X(t)$
X_e
f_e
$1/f_e$
(a) (b) (c) (d) (e)
S

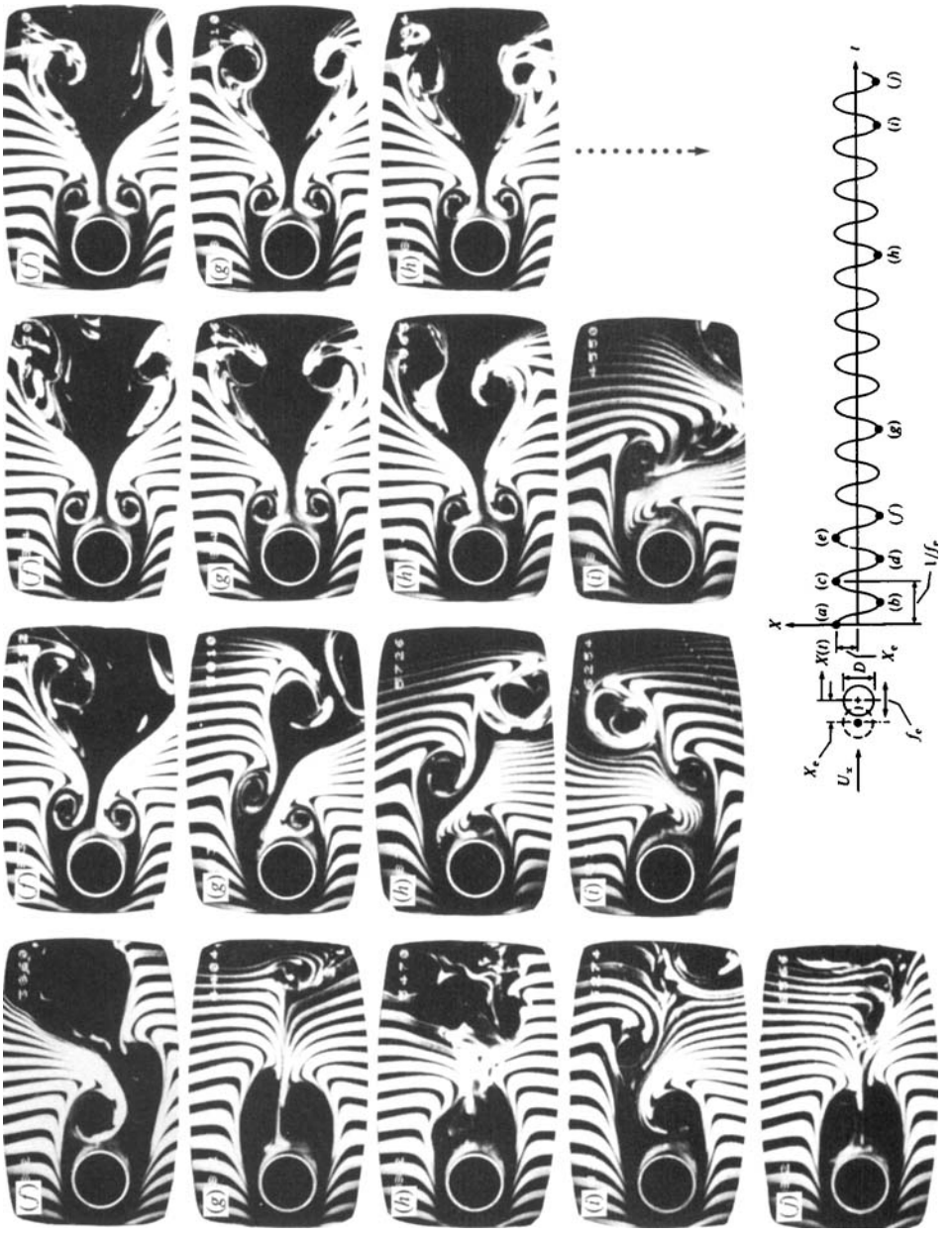

FIGURE 9. Flow structure arising from the onset, and subsequent periodic motion, of cylinder oscillating in streamwise direction ($\alpha = 0°$) as function of ratio of excitation frequency f_e to frequency f_0^* of vortex shedding from corresponding stationary cylinder. (*a*) $t/T_e = 0$; (*b*) 0.5; (*c*) 1.0; (*d*) 1.5; (*e*) 2.0; (*f*) 2.5; (*g*) 3.0; (*h*) 3.5; (*i*) 4.0; (*j*) 4.5.

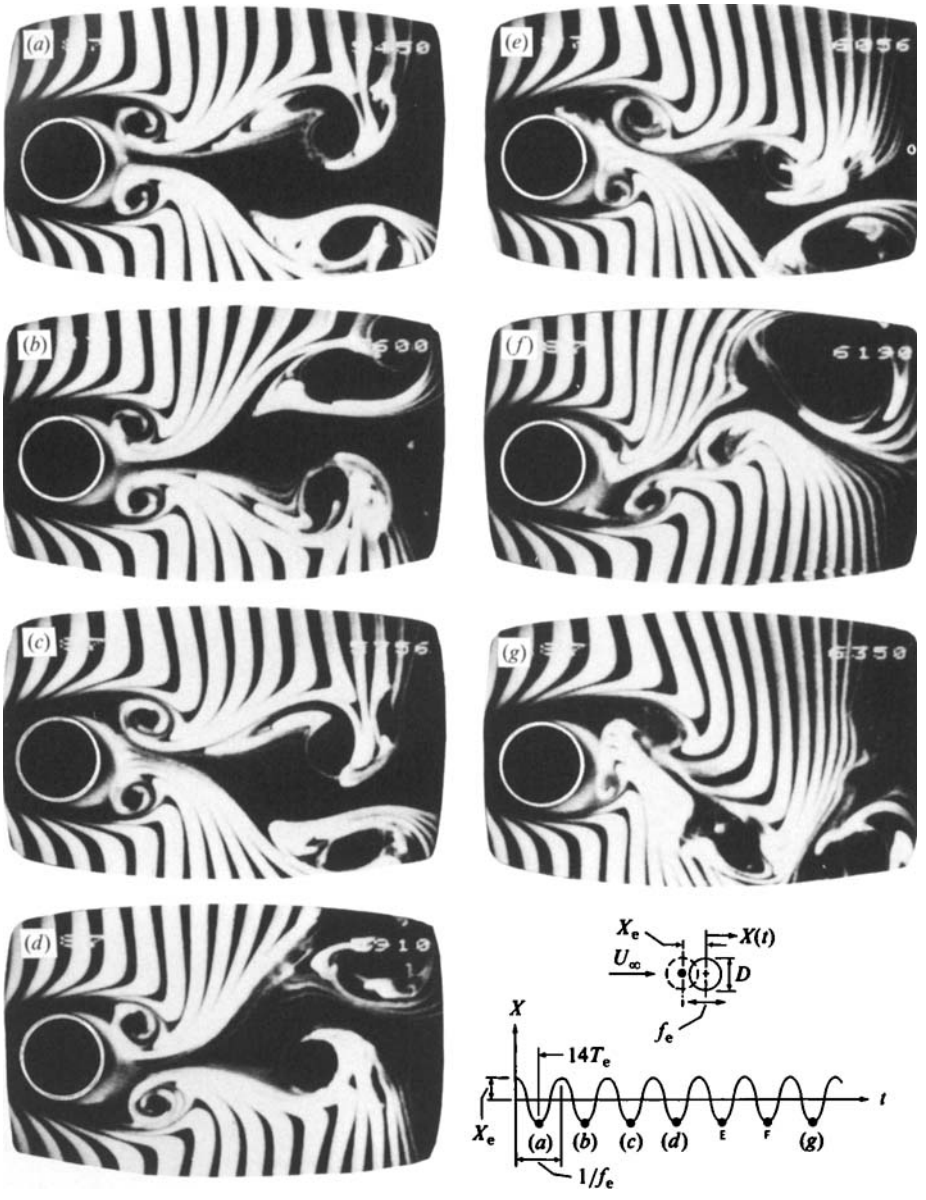

FIGURE 10. Ordered decay of symmetrical S mode of vortex shedding to antisymmetrical A mode for oscillations of cylinder in streamwise ($\alpha = 0°$) direction. Cylinder was abruptly set into streamwise periodic motion at time fourteen cycles prior to upper left photo.

frequency f_e/f_0^*. The number of cycles of symmetric shedding shows a rapid increase in approaching the synchronization condition at $f_e/f_0^* = 1.88$. Similar, deterministic trends of N_S were observed for lower amplitudes $X_e/D = 0.01$, 0.13 (Ongoren 1986). Considering the plot of figure 11 in conjunction with the visualization of figure 9, we conclude that there is a well-defined 'memory effect', defined as the number of cycles for which the initially induced symmetrical mode retains its identity before degenerating to the antisymmetrical mode.

Taking the observations in figures 9–11 as a whole, the question arises as to how

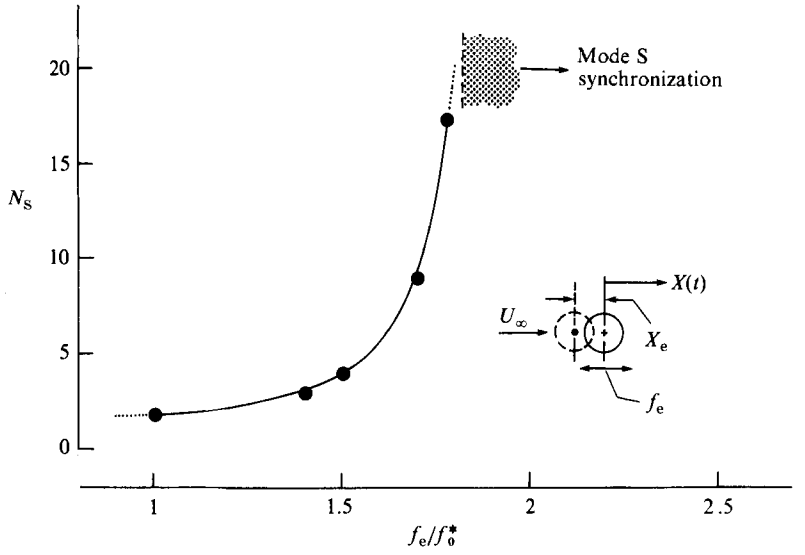

FIGURE 11. Number of cycles of large-scale symmetrical vortex shedding, N_S, prior to onset of antisymmetrical mode of vortex shedding, as a function of excitation frequency f_e/f_0^*. $X_e/D = 3.0$, $\alpha = 0°$.

the downstream vortex dynamics influences the transition from symmetrical to antisymmetrical modes. Visualization of this downstream region showed that the synchronized symmetrical mode, occurring at $f_e/f_0^* = 1.88$, is associated with a downstream row of symmetrical vortex pairs – at least seven or eight consecutive pairs were visible in the restricted field of view downstream of that in figure 9. As a consequence of this downstream symmetry, there is no basis for antisymmetrical upstream influence. On the other hand, at lower values of excitation frequency, where there is transition from a symmetrical to an antisymmetrical mode, the downstream vortex pattern eventually becomes severely antisymmetrical after the onset of cylinder motion. In the region downstream of that shown in figure 9, the first few symmetrical vortex pairs produced at the onset of cylinder motion initially tilt towards antisymmetry. Through mutual induction effects, this tilting is amplified to a pattern of highly antisymmetrical vortex pairs; this pattern simulates mode A-IV. In the final stage, this antisymmetrical vortex pattern creeps upstream, eventually bringing the initially formed vortices from the cylinder into an antisymmetrical mode. The total time taken for onset of the antisymmetrical arrangement of vortices and the decay of the initially shed vortices to antisymmetrical form is a function of frequency ratio f_e/f_0^*, as indicated in figure 11. It is this time-dependent build-up of antisymmetry in the downstream wake region and its upstream influence that makes the transition from symmetrical to antisymmetrical shedding from the cylinder occur with a time lag. This mechanism is distinctly different from that observed for steady-state excitation, described in the first part of this paper. In other words, the initial conditions are central in determining whether the transition between modes will be an abrupt switching, as was observed for steady-state excitation, or a gradual transition, as observed for transient initial conditions.

6. Concluding remarks

A cylinder undergoing controlled oscillations at arbitrary angle α with respect to the free-stream simultaneously induces symmetrical and antisymmetrical perturbations. In addition to these perturbations induced by the cylinder motion, there will be perturbations from the downstream wake region that are felt in the vicinity of the cylinder. These latter perturbations can be communicated upstream through two basic mechanisms: Biot–Savart induction from the downstream vortex array; and wave reflection from a local region of absolute instability providing upstream-travelling perturbations. For the naturally occurring vortex street, both of these types of upstream influence will exert an antisymmetrical perturbation in the near-wake region. Therefore, even in the case of purely symmetrical or antisymmetrical perturbations induced by the cylinder, one must contend with simultaneous excitation in the antisymmetrical mode arising from the downstream dynamics. Clearly, the degree of predominance of these classes of perturbations, relative to each other, depends not only upon their relative amplitudes, but also on their frequencies relative to those of the instability of the near wake.

The coexistence of these two basic types of excitation, that arising from the cylinder motion and that from the upstream influence, provides a rich array of admissible modes of vortex formation from the oscillating cylinder. Moreover, these modes either can be synchronized, i.e. phase-locked, with the cylinder motion, or they can compete with each other. Particularly remarkable is the occurrence of synchronized vortex formation in the antisymmetrical mode when the cylinder motion produces purely symmetrical perturbations of relatively large amplitude.

When mode competition occurs, there is transition back and forth between symmetrical and antisymmetrical modes of vortex formation. The number of occurrences of each mode over a long time is a well-ordered function of excitation frequency and angle α. An important feature of this mode competition is the abrupt switching between antisymmetrical and symmetrical modes; the transition between them takes, at most, two cycles of the cylinder oscillation. This abrupt switching is associated with quasi-synchronization in the antisymmetrical and symmetrical modes. That is, each mode of vortex formation is synchronized until it switches to another, instead of showing a gradual alteration from one mode to another.

In order to examine the effect of initial conditions on the mode competition and transition between modes, the cylinder initially at rest was abruptly set into sinusoidal motion in the streamwise direction. In this case, the initial mode of vortex formation is a symmetrical one. It is followed by decay to an antisymmetrical mode unless the excitation frequency is sufficiently high to produce synchronization in the long-term sense. The number of cycles of symmetrical vortex production before onset of decay into the antisymmetrical mode occurs is a deterministic and repeatable function of excitation frequency. Moreover, the decay from the symmetrical to antisymmetrical mode is a gradual one, typically taking seven or eight cycles of the cylinder oscillation. This transition between modes sharply contrasts with the abrupt switching observed for the case of steady-state excitation of the cylinder. This relatively long time, i.e. large number of cycles, required for the transition from symmetrical to antisymmetrical modes is associated with time-dependent build-up of a large-scale antisymmetrical vortex arrangement in the downstream region of the flow. In essence, the longer it takes for this large-scale vortex array to rearrange into an asymmetrical pattern and migrate upstream, the larger the number of cycles required for onset of decay to the antisymmetrical mode of shedding from the cylinder.

The authors wish to express their appreciation to the Office of Naval Research for primary support of this investigation. During the early part of the study, supplemental funding was received from the Volkswagen Foundation.

REFERENCES

GRIFFIN, O. M. & RAMBERG, S. E. 1976 Vortex shedding from a cylinder vibrating in line with an incident uniform flow. *J. Fluid Mech.* **75**, 257–271.

NAUDASCHER, E. 1986 Flow-induced streamwise vibrations of structures: Parts I and II. *J. Fluids Structures* (in press).

ONGOREN, A. 1986 Unsteady structure and control of near-wake. Ph.D. dissertation, Department of Mechanical Engineering and Mechanics, Lehigh University, Bethlehem, Pennsylvania.

ONGOREN, A. & ROCKWELL, D. 1988 Flow structure from an oscillating cylinder. Part 1. Mechanisms of phase shift and recovery in the near wake. *J. Fluid Mech.* **191**, 197–223.